Pion-nucleus scattering

Mutazz Nuseirat and M. A. K. Lodhi
Texas Tech University, Lubbock, Texas 79409

W. R. Gibbs
New Mexico State University, Las Cruces, New Mexico 88003

(Received 3 February 1998)

An energy-dependent analysis of elastic scattering of π^+ from ^{12}C, ^{16}O, and ^{40}Ca is made based on differential cross sections and (in one case) reaction cross sections. A nonlocal optical model is used to provide the energy variation between data sets. Structure is found in the s- and p-wave phase shifts. [S0556-2813(98)05107-3]

PACS number(s): 13.75.Gx, 25.80.Gn

I. INTRODUCTION

It was pointed out a few years ago [1] that optical models for low-energy pion-nucleus scattering contain poles in the s-matrix which could lead to observable effects in elastic scattering and reactions. These resonances can lead to rapid changes in the cross sections for certain reactions, notably pion double-charge exchange [2,3]. At the time of Ref. [1] only qualitative estimates of the size and location in energy of possible visible manifestations of these structures predicted by the optical model were possible. This work motivated a measurement of the reaction and total cross sections at low energy [4]. No rapid variation in energy was seen in the cross sections measured in this work.

A number of experiments were carried out with the BGO ball [5] at LAMPF (Clinton P. Anderson Meson Physics Facility) with the view of obtaining absorption cross sections in small energy steps. In one experimental setup the elastic scattering from ^{12}C was also measured [6] in small energy steps from 18 to 44 MeV. The BGO ball was not well suited for the measurement of elastic differential cross sections, mostly because of the poor angular resolution (individual crystals were of the order of 30° in extent). Nonetheless, these data provide information not available before, regarding the question raised above.

In this paper we present (for ^{12}C) an analysis based on these points plus the previously measured angular distributions at isolated individual energies as well as the measurements of the reaction cross section [4,7]. For ^{16}O and ^{40}Ca we present an analysis based on measured angular distributions alone.

The interest in such an analysis is (at least) twofold. First, the properties of the propagation of hadrons in nuclear matter are fundamental. Second, knowledge of the wave functions generated by a realistic model of the interaction is needed to predict the reaction cross section in specific channels. Recently it has been claimed [8] that an enhancement seen in measured pion double-charge exchange reactions at low energy provides evidence for the existence of a dibaryon. Since the calculation of these cross sections without the inclusion of a dibaryon [2,3] displays an enhancement in the cross section in the energy region where the peak in the experimental data occurs, it is of great interest to determine if the data can be reproduced without the need of the extra degrees of freedom implied by the introduction of a dibaryon. A crucial step toward a realistic calculation of the double-charge exchange cross section is the determination of pion wave functions consistent with measured elastic scattering cross sections. The optical model used in this paper is similar to that given before [9], but with the improvements given in the next section.

We make a fit to each nucleus (for all energies included) by minimizing a χ^2 constructed as the sum of the individual χ^2 for the elastic data points plus the χ^2 corresponding to renormalization factors for the data plus (for carbon only) the χ^2 from the reaction data. The values of χ^2 obtained are respectable considering the difficulty of the solution of the many-body problem and the quality of the data. The problems of the data have, no doubt, deterred researchers from attempting a fit over a wide energy range. As we shall see, there are still problems of inconsistent data and one must make choices and eliminate points in order to find a useful fit.

II. OPTICAL MODEL

The optical model used in this work [9] incorporates the effects of the medium including Pauli blocking. It has been used [10] successfully in describing scattering from the calcium isotopes in the resonance region. The application of such a model is more challenging at low energies since the pion penetrates deeply into the nucleus.

A new feature of the model, used for the first time in this work, is the possibility of giving each of the six pion-nucleon partial waves needed at low and intermediate energies a different off-shell range corresponding to a different spatial extent of the interaction.

In a recent analysis [11,12] of pion-nucleon scattering it was seen that the ranges of the potentials corresponding to different spins and isospins were distinct. Previous versions of the pion-nucleus optical model assumed the same range for all partial waves (or possibly two ranges, one for s waves and one for p waves).

In the present model we have allowed a different range for each of the six partial waves. The pion-nucleon model mentioned above allowed two potential terms (thus two

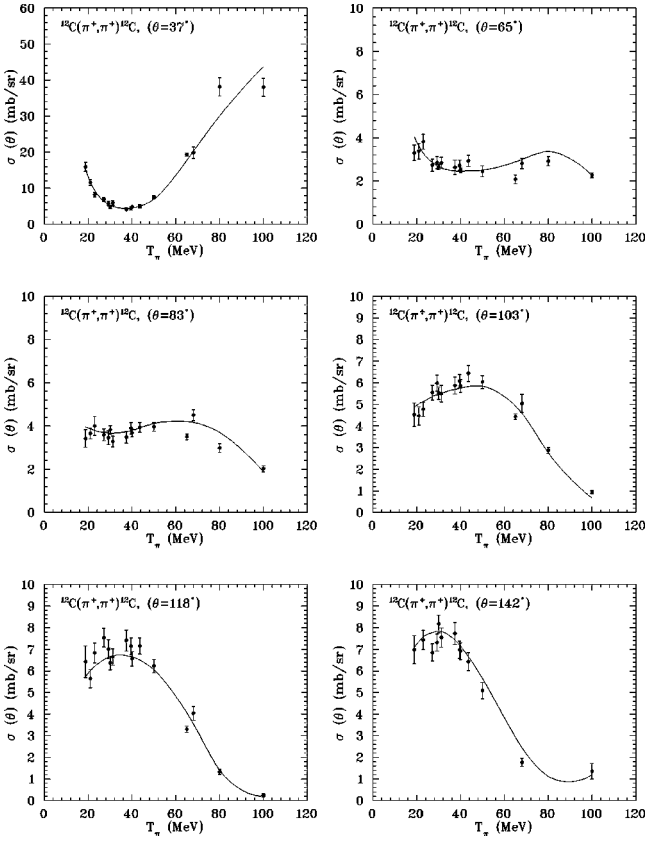

FIG. 1. Fits to the cross sections for ^{12}C. The points at 65 MeV were not included in the fit.

strengths and two ranges) for each of these partial waves (although only one was needed in two of the waves) so that the present model is still restrictive in this sense. Since the pion-nucleon model [12] used an exponential local potential and the present optical model is based on a separable Yamagouchi (π-N) potential, it is not expected that the ranges should correspond exactly. However, we might expect the sizes to roughly track each other.

The technique for the construction and solution of the optical model has been given elsewhere [13], and so we present only a very brief summary here.

The potential for each partial wave is constructed from a first-order optical model given by

$$V_j(\mathbf{q},\mathbf{q}')=f_j(\mathbf{q},\mathbf{q}')S(|\mathbf{q}-\mathbf{q}'|), \tag{1}$$

where $f_j(\mathbf{q},\mathbf{q}')$ is the pion-nucleon amplitude for a given partial wave, labeled by j, with the form

$$f_j(\mathbf{q},\mathbf{q}')=b_j v_j(q)v_j(q')(\mathbf{q}\cdot\mathbf{q}')^l, \tag{2}$$

where l is the angular momentum corresponding to the partial wave j and

$$v_j(q)=\frac{k^2+\alpha_j^2}{q^2+\alpha_j^2}. \tag{3}$$

The quantity $S(|\mathbf{q}-\mathbf{q}'|)$ is the Fourier transform of the density. We calculate separately the neutron and proton densities and hence can calculate a neutron and proton optical potential in the same general manner as in Ref. [10]. Since the difference in the neutron and proton densities is very small for these nuclei, this is not expected to play a significant role. Calculations were performed for several neutron and proton densities with the neutron and proton densities being obtained from the same strong-interaction well. Among these various densities, we chose the one giving the lowest χ^2. The resulting radii were close to, but distinct from, the electron scattering results, unlike in Ref. [10].

These potentials are then transformed into coordinate space to provide nonlocal potentials and the appropriate spin-isospin sums are taken to provide a pion-nucleus potential. The truncated Klein-Gordon equation is then solved by matrix methods as has been explained [13]. This potential contains a finite-range π-N interaction and thus might come under the heading of what has been called a ''momentum-space'' optical potential, even though it is solved in coordinate space.

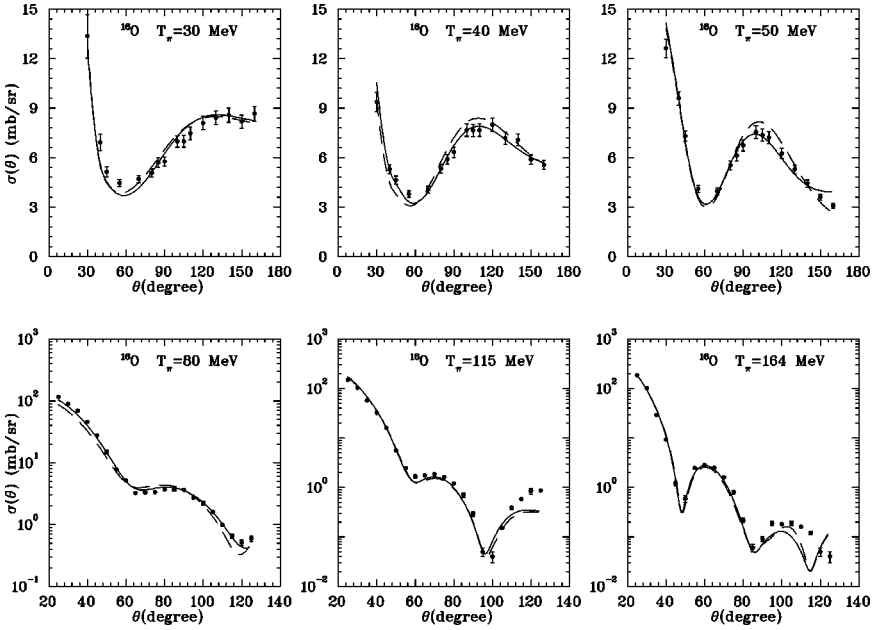

FIG. 2. Fits to the cross sections for ^{16}O. The solid curves show the results of the fit using the parameters determined for ^{16}O and the dashed curves those using the parameters for ^{40}Ca.

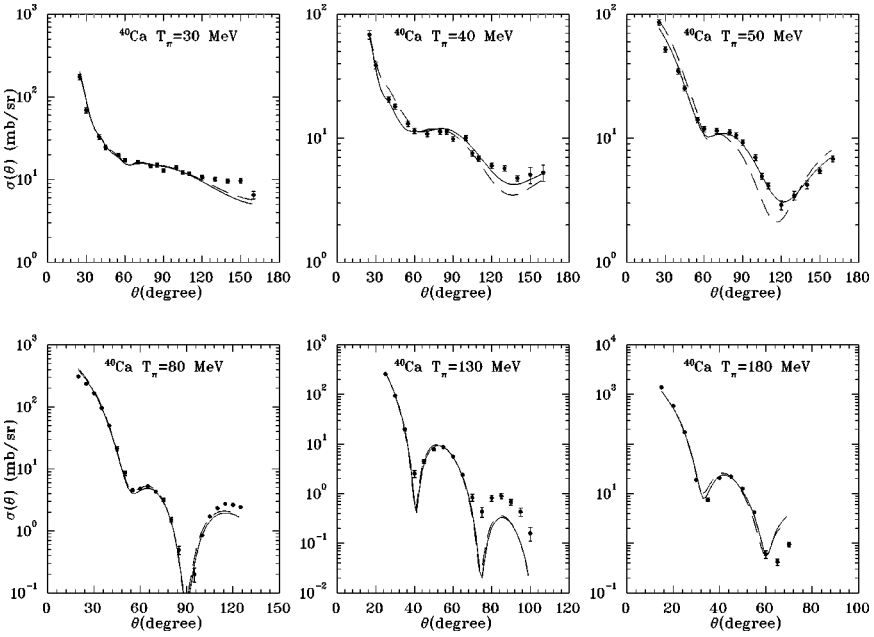

FIG. 3. Fits to the cross sections for ^{40}Ca. The solid curves show the results of the fit using the parameters determined for ^{40}Ca and the dashed curves those using the parameters for ^{16}O.

The strength parameters b_j are calculated starting from free pion-nucleon phase shifts by including the medium corrections of Ref. [9]. Since the calculation is very sensitive to these strengths and the medium corrections cannot be expected to be exact, two multipliers were fit in the analysis, one for the strengths arising from the pion-nucleon s-wave and one from the p-wave strength. These multipliers were found to be of order unity.

The ''true'' absorption (that arising from the actual disappearance of the pion, rather than the excitation of the nucleus) was included with a (purely imaginary) local term in the potential proportional to the product of the proton and neutron density. The coefficient as a function of energy was determined [14] by comparing with measurements of the pion absorption channel [15]. The form obtained for ^{12}C is

$$W_{\rm abs}=46.35\frac{\Gamma^2/4}{(E-E_0)^2+\Gamma^2/4}, \tag{4}$$

where $E_0=215$ MeV and $\Gamma=77$ MeV. The units are fm^4 and this factor is to be multiplied by the square (or product) of densities normalized as

$$\int_0^\infty r^2 dr\rho(r)=1. \tag{5}$$

This factor is assumed to scale as the mass of the nucleus squared.

Since this estimation of the strength of the absorption term cannot be expected to be very accurate, a constant multiplier was fit in the analysis. This multiplier was found to be of order unity.

III. ANALYSIS

In fitting the data, a χ^2 function was constructed which consisted of the sum of two terms. The first was obtained from the theory and experimental values for the differential cross section and errors. The second term was derived from the difference of the normalization (considered as a parameter to be fit and multiplied by the data before the first term was calculated) compared with unity and divided by the experimental estimate of the normalization error. In the case of carbon there was a third contribution constructed from the reaction cross section data. The theoretical parameters and normalizations to the data were then varied to obtain a global minimum in this χ^2.

A. ^{12}C

The BGO ball data [6] provide a set of points in small energy steps over a substantial energy range below 50 MeV. These data show a strong excursion toward smaller values for two to three energies at angles near 90°. The present model was not able to reproduce this very rapid dependence in energy and those points were not included in the analysis.

To supplement these data, previously measured angular distributions were used at 30 [16], 40 [17], 50 [16,18,19], 65 [20], 67.5 [21], 80 [20], and 100 [22] MeV.

At 50 MeV a significant discrepancy among measurements has existed in the past. The latest data seem to show agreement and the numbers from Ref. [18] were used.

The two measurements around 65 MeV differ by as much as a factor of 2 even though they are separated by only 2.5 MeV in energy. The measurement by Amann *et al.* [21] (the higher of the two) has a normalization error of 20% which

TABLE I. Ranges from the fits to the data.

Partial wave	α_j (MeV) ^{12}C	α_j (MeV) ^{16}O	α_j (MeV) ^{40}Ca	α_j (MeV) Ref. [12]
S_1	142	174	147	310.5, 748.9
S_3	1128	1533	556	722.9, 487.0
P_{11}	363	389	343	720.4
P_{31}	443	561	237	630.3
P_{13}	313	562	173	528.7, 814.0
P_{33}	1037	1157	1207	891.7, 486.7

TABLE II. Normalizations for the fits to the data.

^{12}C	Normalization	^{16}O	Normalization	^{40}Ca	Normalization
30 MeV	0.90	30 MeV	0.82	30 MeV	0.74
40 MeV	1.00	40 MeV	0.87	40 MeV	0.90
50 MeV	0.93	50 MeV	0.94	50 MeV	1.11
67.5 MeV	1.06	80 MeV	1.35	80 MeV	1.00
80 MeV	1.18	114 MeV	0.84	130 MeV	1.03
100 MeV	0.76	164 MeV	1.00	180 MeV	1.16
BGO ball	0.88				

can explain a part of the discrepancy. Nonetheless, it seems likely that the other measurement is too low and we find that a renormalization up is required. Since the BGO ball data consist of cross sections at six angles as a function of energy, the fits were made only at those angles for the other data as well, with some interpolation being needed. The fits shown here include the 67.5 MeV data and not that from 65 MeV (investigations made with the opposite choice showed similar results to those given here). The reaction cross section data [4,7] at energies 30, 40, 50, and 65 MeV were also included in the fit. The fits to the six angles are shown in Fig. 1.

The χ^2 for the global fit was 142.9 for 89 data points, 6.9 for 4 reaction cross sections, and 16.9 for 7 normalizations.

The reaction cross section was especially important in distinguishing fits. A second fit was possible to the elastic data only, with different parameters for the optical model. This second fit had stronger variations in the phase shifts than those observed in the present fit (see below), but failed completely to describe the reaction cross section data. The root mean square radius of the proton density was 2.18 fm to be compared with the (proton size corrected) electron scattering value of 2.32 fm.

B. ^{16}O

For ^{16}O a larger energy range was attempted, going to 164 MeV. We used data at 30 [16], 40 [17], 50 [16], 80, 115, and 164 [25] MeV. At the higher energies a fit to the cross section beyond the third maximum was not attempted (although the points are shown on the graphs in Fig. 2). Data points not included in the fit were the largest angle point at 50 MeV and the last five and last seven points at 115 and 164 MeV, respectively.

The fit was initiated with the values of the parameters found for the carbon case and only differential cross section data were used. The total χ^2 was 363 for 98 data points and 22 for the 6 normalizations. Several densities were used with a minimum χ^2 being determined for each one. The best fit is shown here and corresponds to a proton radius of 2.44 fm and a neutron radius of 2.40 fm. The value from electron scattering is 2.58 fm in this case.

TABLE III. Scaling factors for the fits.

Multiplier	^{12}C	^{16}O	^{40}Ca
Absorption	0.91	0.87	0.45
s wave	1.50	1.30	1.30
p wave	1.20	1.19	1.16

C. ^{40}Ca

In the case of ^{40}Ca we attempted a fit up to 180 MeV (see Fig. 3). We used data at 30 [16], 40 [17], 50 [16], 80 [26], 130, and 180 [27] MeV. Again, cross section points at the largest angles were not included. Data points omitted were (a) 30 MeV: 90°, 130°, 140°, and 150°. The point at 90° appears far out of line and the other three points could not be fit within our model (b) 40 MeV: 130°. (c) 50 MeV: none. (d) 80 MeV: the last 5 points. (e) 164 MeV: The last 6 points. (f) 180 MeV: the last 2 points. The χ^2 was 304 for 89 points and 12 for 6 normalizations.

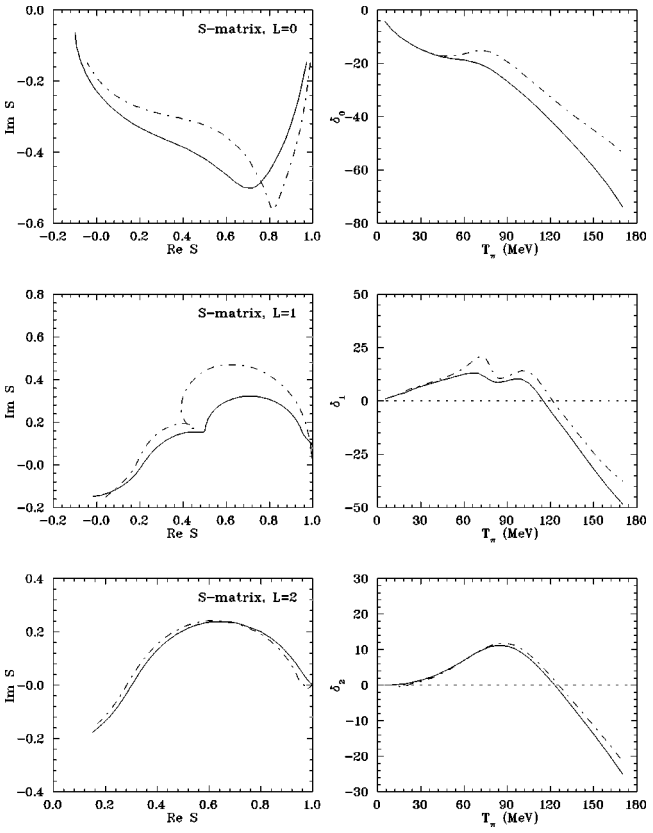

FIG. 4. π-nucleus *s*-, *p*-, and *d*-wave phase shifts for ^{12}C as a function of energy. The dash-dotted curve shows the result of removing the true absorption.

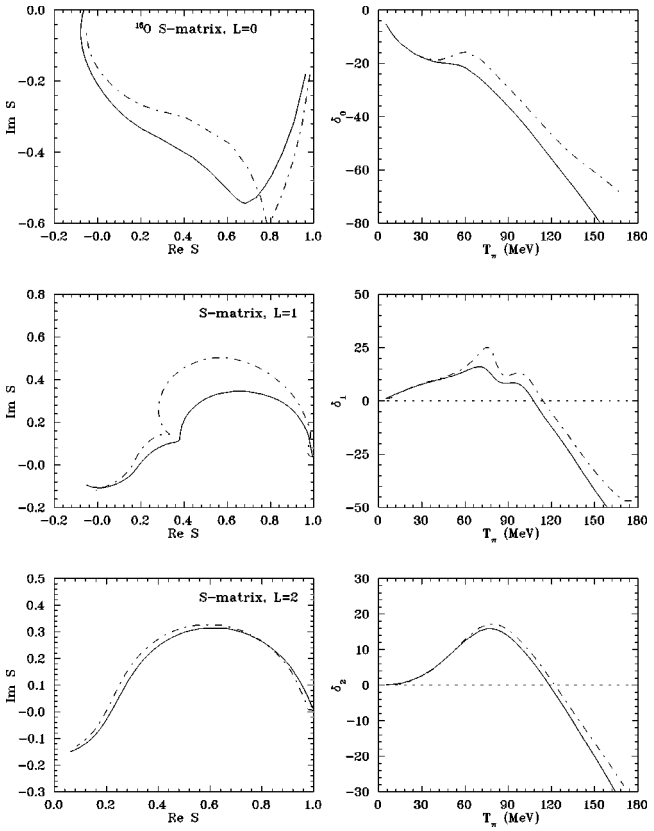

FIG. 5. π-nucleus s-, p-, and d-wave phase shifts for ^{16}O as a function of energy. The meaning of the curves is the same as in Fig. 4.

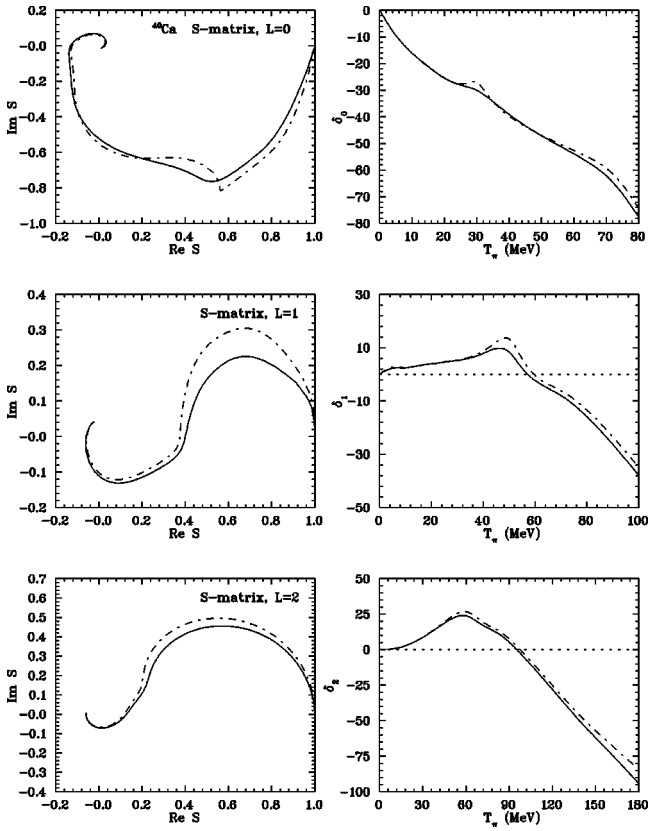

FIG. 6. π-nucleus s-, p-, and d-wave phase shifts for ^{40}Ca as a function of energy. The meaning of the curves is the same as in Fig. 4.

IV. RESULTS

The cross sections do not show any rapid variation with energy, although there is some gentle structure. The scattering model would be more useful if there were a universal set of parameters for all nuclei. Since the corrections to the ranges and multipliers are expected (at least partially) to arise from effects such as Pauli blocking which vary from nucleus to nucleus, such a simple notion must break down at some point. A simple check on this idea is provided by using the parameters fit to ^{16}O to predict ^{40}Ca and vice versa. The dashed curves on the cross section comparisons with the data in these two cases are calculated with the parameters obtained from the fit to the conjugate nucleus. It is seen that the largest differences occur at 40 and 50 MeV.

A. Ranges

The values of the six ranges found by fitting are shown in Table I. The most important ranges (in the sense of sensitivity) were those corresponding to the S_1 and P_{33} waves. The others were poorly determined. It is somewhat surprising that the S_1 is so small and the P_{33} is so large.

Also included in the same table for comparison are the ranges from Ref. [12]. Since those values were derived from π-N scattering with a local exponential potential only, a rough correspondence can be expected.

B. Normalization

The three lowest-energy data sets were taken at a time when the Karlsruhe-Helsinki phase shifts [23] provided standards of normalization. Since these phase shifts were obtained from the Bertin data [24] at 30, 40, and 50 MeV, it should not be surprising if these nuclear cross sections turn out to be somewhat too large. References [11,12] discuss the new measurements and the discrepancy in the pion-nucleon case.

Shown in Table II are the normalizations found for the different data sets.

C. Multipliers

The absorption factor multipliers (see Table III) are all observed to be less than unity, showing that the estimate coming from the absorption cross sections is slightly too large. The fact that it decreases with increasing mass number indicates that the scaling with mass squared is too strong, but of the right order. This absorptive potential, calculated by the squaring rule, changes by more than an order of magnitude from carbon to calcium.

The factors for the s and p waves are of the order predicted from the ''angle transform.'' A crude model [28] would give the multiplier for the p wave to be $1+\mu/m \approx 1.14$ at low energy. The s-wave multiplier is expected to be larger (up to a factor of 2) but these estimates are based on low-energy considerations, whereas the present fit is over a larger energy range.

D. Phase shifts

From the representation of the S matrix as

$$S_l = \eta_l e^{2i\delta_l}$$

with η_l and δ_l real, the phase shifts can be obtained.

The s-, p-, and d-wave phase shifts are shown in Figs. 4, 5, and 6. The solid curves are calculated with the inclusion of the true absorption contribution to the potential, while the dash-dotted curves omit it to show more clearly the resonance behavior. A universal feature of the phase shifts is a strong negative trend as the resonance region is approached. This is to be expected, since for a purely absorbing nucleus the wave function must be zero at the surface; hence the phase shifts must resemble those of a hard sphere. Of course, the surface of the nucleus is not sharp; so the comparison with a hard sphere is only qualitative.

The s-wave phase shifts for all three nuclei clearly show a remnant of the effect suggested in Ref. [1]. The phase shift starts to rise to pass through zero (which would correspond to transparency for the s wave at that energy) but then suffers the influence of the absorption and descends rapidly. In the Argand plot the global behavior is a clockwise movement, but at around 35–50 MeV (the minimum in the figure) there is a sudden change of direction to counterclockwise which is an indication of a resonance behavior. The p-wave phase shift shows a clear indication of an inelastic resonance around 80 MeV for all three nuclei.

V. CONCLUSIONS

We have obtained a fit to data over a substantial energy range for three nuclei with a nonlocal, finite-range optical model. The results show highly damped resonance behavior in the s and p waves for all three nuclei.

It is natural to ask if these are the correct phase shifts for pion scattering from these nuclei. To say they are would, perhaps, be too strong a claim. What is found is that, *for this model*, those are the phase shifts. From arguments from Ref. [1], where it was shown that these types of resonances are present in a range of Kisslinger potential models (including a square well and a potential with a diffuse surface), it seems that the same type of behavior can be expected for many of the various optical models that have been used to describe the scattering of pions from nuclei over the years.

To deny the correctness of the qualitative behavior of the phase shifts one must question the validity of the use of a mean field model for the scattering of pions, or at least the use of a Kisslinger-type model to represent the mean field. These considerations raise more difficult questions and the conventional wisdom is that such mean field approaches are appropriate.

Hence it seems very likely that structures of this type are real. The extraction of their exact position and shape will be model dependent to some extent. The best test of their existence may well be the calculation of reaction cross sections, such as those for double-charge exchange.

This work was supported by the U.S. Department of Energy.

[1] W. R. Gibbs, W. B. Kaufmann, and J. P. Dedonder, Phys. Lett. B **231**, 6 (1989).
[2] N. Auerbach, W. R. Gibbs, Joseph N. Ginocchio, and W. B. Kaufmann, Phys. Rev. C **38**, 1277 (1988).
[3] M. J. Leitch, in *Proceedings of ''Fundamental Symmetries and Nuclear Structure,''* Santa Fe, 1988, edited by J. N. Ginocchio and S. P. Rosen (World Scientific, Singapore, 1989).
[4] A. Saunders *et al.*, Phys. Rev. C **53**, 1745 (1996).
[5] E. A. Pasyuk *et al.*, Phys. Rev. C **55**, 1026 (1987).
[6] M. Yu. Alexakhin *et al.*, Phys. Rev. C **57**, 2409 (1998).
[7] O. Meirav, E. Friedman, A. Altman, M. Hanna, R. R. Johnson, and D. R. Gill, Phys. Rev. C **36**, 1066 (1987); O. Meirav, E. Friedman, R. R. Johnson, R. Olszewski, and P. Weber, *ibid.* **40**, 843 (1989).
[8] R. Bilger, H. Clement, and M. G. Schepkin, Phys. Rev. Lett. **71**, 42 (1993); **72**, 2972 (1994).
[9] W. B. Kaufmann and W. R. Gibbs, Phys. Rev. C **28**, 1286 (1983).
[10] W. R. Gibbs and J.-P. Dedonder, Phys. Rev. C **46**, 1825 (1992).
[11] W. R. Gibbs, Li Ai, and W. B. Kaufmann, Phys. Rev. Lett. **74**, 3740 (1995); πN Newslett. **2**(11), 84 (1995).
[12] W. R. Gibbs, Li Ai, and W. B. Kaufmann, Phys. Rev. C **57**, 784 (1998).
[13] W. R. Gibbs, *Computation in Modern Physics* (World Scientific, Singapore, 1994).
[14] Maher ElGhossain, Ph.D. thesis, Texas Tech University, 1996.
[15] D. Ashery *et al.*, Phys. Rev. C **23**, 2173 (1981); K. Nakai *et al.*, Phys. Rev. Lett. **44**, 1446 (1980); R. D. Ransome *et al.*, Phys. Rev. C **46**, 273 (1992).
[16] B. M. Preedom *et al.*, Phys. Rev. C **23**, 1134 (1981).
[17] M. Blecher *et al.*, Phys. Rev. C **20**, 1884 (1979).
[18] R. J. Sobie *et al.*, Phys. Rev. C **30**, 1612 (1984).
[19] B. G. Ritchie *et al.*, Phys. Rev. C **41**, 1668 (1990).
[20] M. Blecher *et al.*, Phys. Rev. C **28**, 2033 (1983).
[21] J. F. Amann *et al.*, Phys. Rev. C **23**, 1635 (1981).
[22] L. E. Antonuk *et al.*, Nucl. Phys. **A420**, 435 (1984).
[23] R. Koch and E. Pietarinen, Nucl. Phys. **B336**, 331 (1980).
[24] P. Y. Bertin *et al.*, Nucl. Phys. **B106**, 341 (1976).
[25] J. P. Albanese, J. Arvieu, J. Bolger, E. Boschitz, and C. H. Q. Ingram, Nucl. Phys. **A350**, 301 (1980).
[26] M. J. Leitch *et al.*, Phys. Rev. C **29**, 561 (1984).
[27] P. Gretillat, J.-P. Egger, J.-F. Germond, C. Lunke, E. Schwarz, C. Perrin, and B. M. Preedom, Nucl. Phys. **A364**, 270 (1981).
[28] W. R. Gibbs, B. F. Gibson, A. T. Hess, G. J. Stephenson, Jr., and W. B. Kaufmann, Phys. Rev. C **13**, 2433 (1976).